First-principles investigation of amorphous n-type In_2O_3 for BEOL transistor

Yaoqiao Hu[1], Wriddhi Chakraborty[2], Huacheng Ye[2], Suman Datta[2], Kyeongjae Cho[1]

[1]Department of Materials Science and Engineering, University of Texas at Dallas, Richardson, TX 75080, USA
[2]Department of Electrical Engineering. University of Notre Dame, Notre Dame, IN 46556, USA

Email: kjcho@utdallas.edu

Abstract – The electronic transport properties of amorphous In_2O_3 (a-In_2O_3) are investigated from first principles simulations for BEOL transistor application. It is determined that local atomic and electronic structure disorders in a-In_2O_3 are the fundamental origin of reduced mobility in amorphous phase. Medium range order In-In connectivity is responsible for the electron conduction pathway. It is found that amorphous disorder present in a-In_2O_3 could induce shallow donor states and acceptor states that are responsible for the device threshold voltage instability. Nonstoichiometric defects including indium vacancy and interstitial will further increase the density of these defect states intrinsic to a-In_2O_3. The results could provide a better understanding of the electronic transport behavior in a-In_2O_3 and useful insights for future defect controlling for better device performance.

Key words – amorphous oxides, electronic structure, first principles calculations, field effect transistors

I. Introduction

Amorphous oxide semiconductors like In_2O_3 have recently gained revived interests for its great potential in back-end-of-line (BEOL) compatible transistors for monolithic 3D integration.[1] Recent works on amorphous In_2O_3 (a-In_2O_3) based thin film transistors (TFTs) have demonstrated their outstanding device performances.[2,3] However, due to the amorphous nature, a-In_2O_3 is expected to exhibit different electronic transport behaviors from its crystalline counterpart: for example, the presence of structure disorder and nonstoichiometric defect could destabilize the transistor's threshold voltage. W doping is introduced to improve the stability as well as adding electron carriers to a-In_2O_3 leading to amorphous In-W-O (a-IWO) which is experimentally investigated. In this work, we perform density functional theory (DFT) based first-principles simulations on a-In_2O_3 and a-IWO, and compare with experimental data to investigate their electronic transport properties in the context of device applications.

II. Computational methods

Amorphous atomic structure of a-IWO was generated by simulating the experimental melt-quench process [4] using ab-initio molecular dynamics as implemented in VASP. [5, 6] Calculations were based on DFT using plane wave expansion method and GGA-PBE functional. The cutoff energy was set at 420 eV. Atomic structures were relaxed using quasi-Newton algorithm method, with the convergence criterion of the force to be 0.02 eV/Å. For electronic structure calculation, a Blocked-Davidson algorithm was used with the converged energy criterion of 10^{-5} eV. Formation energies of charged defects were calculated by using PyCDT package [7] with Freysoldt correction scheme [8] employed.

III. Results and discussion

Figure 1(a) shows the temperature profile for the melt quench process in our ab-initio MD simulation, with the corresponding atomic structure of a-In_2O_3 shown in **Figure 1(b)**. **Figure 1(c)** plots the radial distribution function (RDF) of O-O, In-In, and In-O pairs. For all pairs, the RDFs exhibit an initial sharp peak and significantly broadened second peak, corresponding to the short-range order and the loss of long range order in a-In_2O_3, suggesting the reasonability of the generated amorphous structure. In **Figure 1(d)**, the coordination numbers of In and O are presented. Comparing to crystalline phase where In has oxygen coordination number (CN) of 6 and O has In CN of 4, a general under-coordination can be observed in amorphous phase due to the local structural distortions.
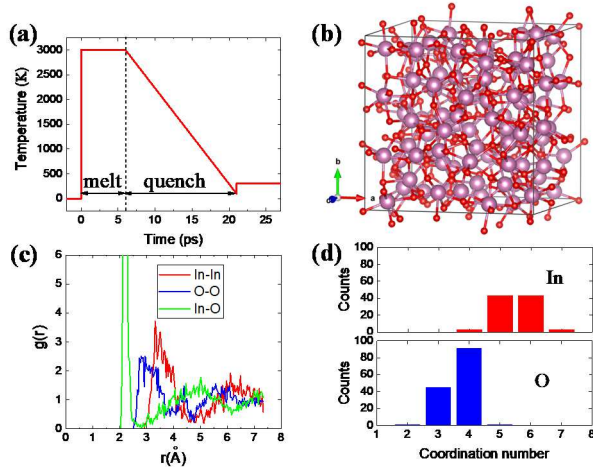
Figure 1 (a) Temperature profile for the melt-quench process used in an-initio MD for generating amorphous atomic structure of In2O3. (b) Schematics of atomic structure of amorphous In2O3. (c) In-In, O-O, and In-O pair radial distribution functions showing the generating amorphous structure retaining short-range disorder but losing long-range order. (d) The statistical distribution of In an O coordination number.

We performed DFT calculations to investigate the localization effect in amorphous phase and its influence on electronic transport properties. **Figure 2(a)** plots the calculated inverse participation ratio (IPR)[9] and density of states (DOS) versus energy position. IPR is a measure of how a specific electronic state spatially distributed over different atoms and a higher value means that electrons are more localized. Based on the exponential scaling relationship between mobility and IPR from our recent work [10], the electron mobility in a-In2O3 is estimated to be in the range of 30~50 cm²/Vs which is consistent with recent experiment work [2]. The electron transport is closely related to the In-In connectivity since the conduction band is dominated by indium 5s orbital. For crystalline phase, In-In connection is mediated by common oxygen corner sharing or edge sharing (**Figure 2c and 2d**). Due to a shorter In-In bonding distance, edge sharing is expected to be more facilitating for electron transport. Upon amorphization, the In-In common oxygen edge sharing breaks down into corner sharing, as evidenced by the In-In connectivity statistical results in **Figure 2b**. The transition from In-In edge sharing connection to In-In corner sharing connection is the underlying reason for mobility reduction in a-

In2O3 and could be generally extended to other metal oxides.
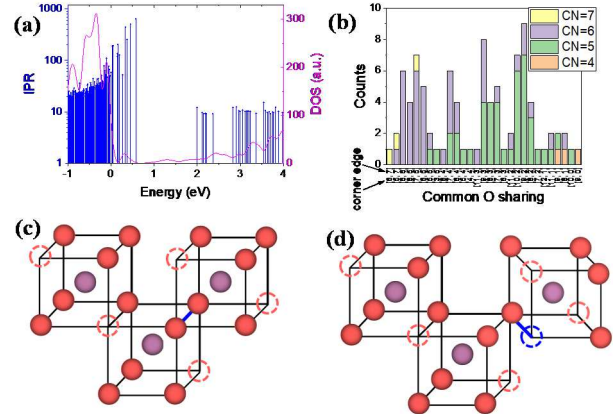
Figure 2 (a) IPR and DOS distribution in a-In2O3. (b) In-In connectivity in a-In2O3. In crystalline phase, each In is coordinated to 12 In atoms, with 6 of them connected by corner shared O and 6 of them by edge shared O. In amorphous phase, a general increase of corner sharing and decrease of edge sharing is observed, meaning that In-In edge sharing connectivity changes to In-In corner sharing. The corresponding atomic structure origin for this change are shown in (c) and (d). (c) atomic structure of c-In2O3 showing how InOx polyhedra are connected to each other by sharing O atoms. (d) Schematics of atomic structure of a-In2O3 showing local structure distortion would lead to edge sharing transition to corner sharing.

Recently, our experimental team members have performed electrical characterization work on amorphous phase W-doped In2O3 (a-IWO) transistors. **Figure 3(a)** shows the schematic of a-IWO channel back-gate transistor. The 7-nm-thick amorphous In2O3 with 1 at% W dopants was deposited by RF-sputtering. **Figure 3(b)** shows gate voltage and drain voltage setup for the electrical stress measurement. **Figure 3(c)** shows that due to the defect gap states the gate bias stress could result in a positive V_{TH} shift and the amount of V_{TH} variation increases with the applied stress time duration. **Figure 3(d)** is the electrical characterization results of the defect gap states including their densities and energetic locations. Two Gaussian-type fitted peaks appear in the sub-gap region, in addition to the tail states. The donor defect states are in the tailing state region close to the conduction band edge (CBE) while the acceptor defect states are located deeper (~0.25eV below CBE). In **Figure 3(e),** the electrical stress caused the acceptor

states increasing and donor states decreasing, which could explain the observed V_{TH} positive shift.
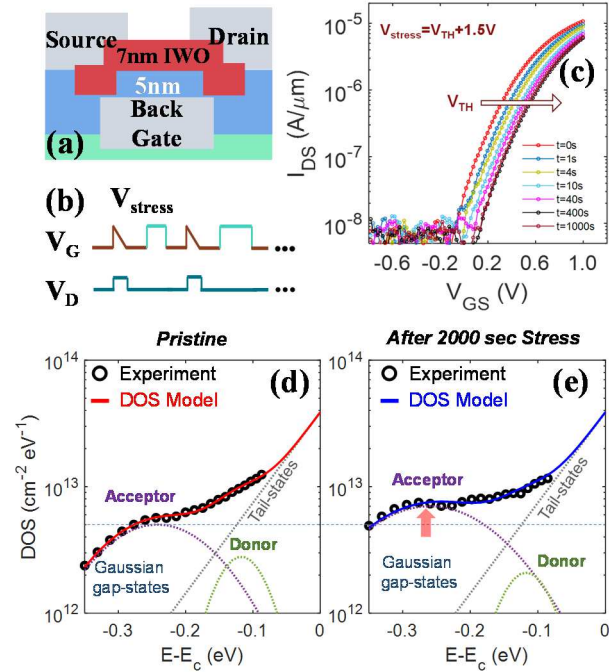
Figure 3 Experimental results on electrical characterization of defect gap states in a-IWO. (a) Schematics of a-IWO device structure. (b) Gate voltage and drain voltage setup in the electrical bias stress measurement. (c) I-V curve of electrical stress measurement. (d) Experimental extracted DOS distribution before stress and (e) after stress.

To elucidate the nature of these gap states as well as to provide insight for better control of the defect gap states for improved device performance, DFT calculations are performed to identify the atomic structural origin of the experimentally observed defect gap states. **Figure 4(c)** shows the calculated DOS for stoichiometric a-IWO (W doping concentration ~1 at%). Three occupied DOS peaks can be observed in the gap region below the Fermi level (E_F) which is the charge neutrality level of the amorphous oxide. The charge density spatial distribution for these three DOS peaks were analyzed, as shown in **Figure 4**. Peak 1 and peak 3 are associated with undercoordinated In, with electrons being localized at the vacant void region which could be viewed as intrinsic oxygen vacancy defects. Peak 2 is associated with the W dopant. For gap states peak 1 and peak 2, electrons are highly localized; while for peak 3 electrons are more delocalized as electron density is distributed throughout a much wider spatial region. In crystalline

IWO, the Fermi level is located within the conduction band forming an extended electron conduction states. In a-IWO, such extended conduction states are partially localized by the atomic disorder leading to the delocalized gap states in peak 3.
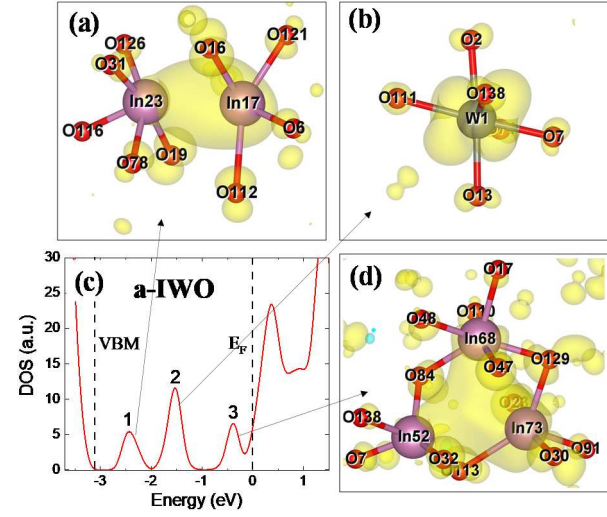

Figure 4 DOS of a-IWO. (c) DFT calculated DOS distribution in the gap region of stoichiometric a-IWO. (a) (b) and (d) are the spatial charge distribution corresponding to three peaks shown in (c).

To examine the role of externally induced defects in the electronic state evolution during the voltage stress as shown in Fig. 3, DOSs of a-IWO with additional point defects including oxygen vacancy (V_O), indium vacancy (V_{In}), and O interstitial (O_i), and indium interstitial (In_i) (referred to as nonstoichiometric defects hereafter) are also calculated. Nonstoichiometric defects introduced into a-IWO overall do not induce prominent new DOS peak as we can see from **Figure 5(a)-(d)** that most of the gap state peaks are overlapping with those of stochiometric a-IWO. Nevertheless, these nonstoichiometric defects will increase the intensity of DOS peaks intrinsic to a-IWO as well as shifting the Fermi level of the DOS which corresponds to V_{TH} shift in the device measurements. By evaluating the Fermi level position shift, it can be determined that V_{In} is an acceptor defect while In_i is a donor defect. O_i and V_O do not induce electron doping or trapping effect as there are negligible Fermi level shifts.
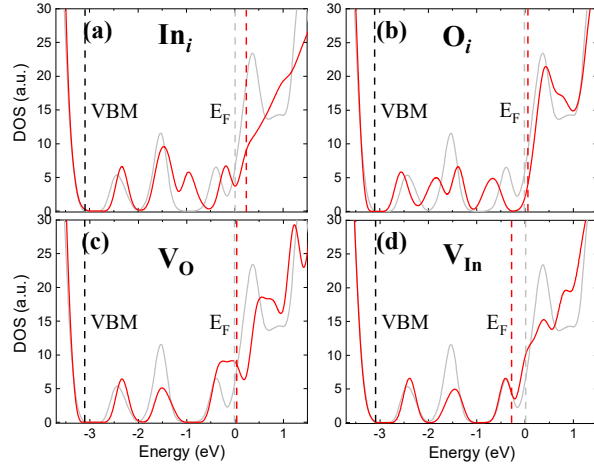
Figure 5 DOS of a-IWO with additional point defects (nonstoichiometric a-IWO). Four intrinsic defects, including (a) indium interstitial (In_i) (b) O interstitial (O_i), (c) oxygen vacancy (V_O), and indium vacancy (V_{In}), are considered.

Gate voltage stress during device operation could induce new defects to form and cause threshold voltage instability. To investigate the possible defect origin for device instability issue, formation energies of various defects were calculated, as shown in **Figure 6.** The applied gate voltage during electrical stress will move the Fermi level above the conduction band, under which most of defects become more negatively charged by accepting more electrons. This suggests that electrical stress will cause additional point defects to form, and these newly formed defects will increase the acceptor states and thus shift the threshold voltage of a-IWO based transistors. This result can explain the experimental observation that in a-IWO based transistor, the threshold voltage suffers from positive shift under positive gate voltage bias stress.
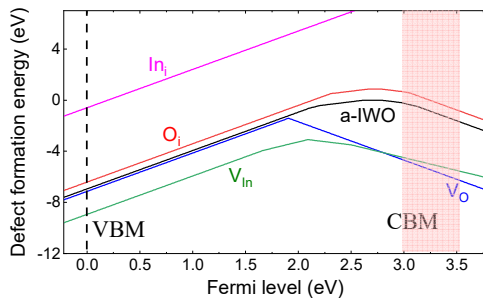
Figure 6 Formation energies of various defects in equilibrium amorphous IWO with density $\rho=6.6g/cm^3$.

In addition to the amorphous disorder and nonstoichiometric defects present within a-In_2O_3, thin film a-In_2O_3 are also subject to interface defects at a-In_2O_3/dielectric (a-HfO_2 in the current device) interface. Given the nano-meter-thick a-In_2O_3 channel, interface defect states are expected to play a significant role in determining the electronic structure and transport properties. The interface model including In_2O_3/HfO_2, In_2O_3/Al_2O_3, and In_2O_3/HZO stack will be our further research work to shed light on their implications on the electron transport properties as well as device performances.

IV. Conclusion

In conclusion, we have performed DFT based first-principles calculations to investigate the electronic state properties of a-In_2O_3 for BEOL transistor application. Amorphous structure generally exhibits under-coordination due to local structure disorder, which leads to localized electronic states as the fundamental origin of reduced mobility in amorphous phase. The defect gap states are intrinsic to stoichiometric W doped a-In_2O_3 and nonstoichiometric defects only act to increase the defect state density. Under electrical stress, these defect states could result in V_{TH} instability. The results would provide a better understanding of the electronic transport behavior in a-In_2O_3 and also some insights on the role of defects in a-In_2O_3 based device operation.

Reference
[1] Salahuddin et al. Nature Electron 2018, 1.8, 442-450
[2] Si et al. Nano Lett. 2021, 21, 500-506
[3] Chakraborty et al. IEEE Trans. Electron Devices 2020, 67(12), 5336-5342
[4] Bruce Buchholz et al. Chem. Mater. 2014, 26, 5401-5411
[5] Kresse et al. Phys. Rev. B 1993, 47, 558
[6] Kresse et al. Phys. Rev. B 1996, 54, 11169
[7] Broberg, et al. Comput. Phys. Commun. 2018, 226, 165
[8] Freysoldt et al. Phys. Status Solidi Basic Res. 2011, 248, 1067-1076
[9] Kaur et al. *Energy Procedia* 2012, 29 291-299
[10] Lee et al. mobility characterization of amorphous semiconductors, under preparation